Nonclassical Titanocene Silyl Hydrides

Stanislav K. Ignatov,[c] Nicholas H. Rees,[b] Ben R. Tyrrell,[b] Stuart R. Dubberley,[b] Alexei G. Razuvaev,[c] Philip Mountford,*[b] and Georgii I. Nikonov*[a]

Abstract: The titanocene silyl hydride complexes $[Ti(Cp)_2(PMe_3)(H)(SiR_3)]$ [SiR_3 = SiMePhCl (**6**), $SiPh_2Cl$ (**7**), $SiMeCl_2$ (**8**), $SiCl_3$ (**9**)] were prepared by $HSiR_3$ addition to $[Ti(Cp)_2(PMe_3)_2]$ and were studied by NMR and IR spectroscopy, X-ray diffraction (for **6**, **8**, and **9**), and DFT calculations. Spectroscopic and structural data established that these complexes exhibit nonclassical Ti-H-Si-Cl interligand hypervalent interactions. In particular, the observation of silicon–hydride coupling constants J(Si,H) in **6**–**9** in the range 22–40 Hz, the signs of which we found to be negative for **8** and **9**, is conclusive evidence of the presence of a direct Si–H bond. The analogous reaction of $[Ti(Cp)_2(PMe_3)_2]$ with $HSi(OEt)_3$ does not afford the expected classical silyl hydride complex $[Ti(Cp)_2(PMe_3)(H)\{Si(OEt)_3\}]$, and instead NMR-silent titanium (apparently Ti^{III}) complex(es) and the silane redistribution product $Si(OEt)_4$ are formed. The structural data and DFT calculations for the compounds $[Ti(Cp)_2(PMe_3)(H)(SiR_3)]$ show that the strength of interligand hypervalent interactions in the chlorosilyl complexes decreases as the number of chloro groups on silicon increases. However, in the absence of an Si-bound electron-withdrawing group *trans* to the Si–H moiety, a silane σ complex is formed, characterized by a long Ti–Si bond of 2.658 Å and short Si–H contact of 1.840 Å in the model complex $[Ti(Cp)_2(PMe_3)(H)(SiMe_3)]$. Both the silane σ complexes and silyl hydride complexes with interligand hypervalent interactions exhibit bond paths between the silicon and hydride atoms in Atoms in Molecules (AIM) studies. To date a classical titanocene phosphane silyl hydride complex without any Si–H interaction has not been observed, and therefore titanocene silyl hydrides are, depending on the nature of the R groups on Si, either silane σ complexes or compounds with an interligand hypervalent interaction.

Keywords: density functional calculations · hydride ligands · hypervalent compounds · silicon · titanium

Introduction

Nonclassical Si–H interactions in transition-metal complexes are currently the subject of intense research.[1] In addition to the well-established σ complexes of silane Si–H bonds $[M(L)_n(\eta^2\text{-H-}SiR_3)]$[1a–e] and Si-H-M agostic interactions,[2–5] a plethora of new types of interligand interactions has been recently discovered.[1f] These include interligand hypervalent interactions (IHI)[6–8] and a variety of multicenter Si–H interactions found in some complexes of Ru and Os, the bonding in which is the subject of continuing debate.[9–12] However, for a given ligand set and metal, usually only one type of Si–H interaction (if any) occurs.

Our present work was stimulated by the report by Buchwald et al. that $[Ti(Cp)_2(PMe_3)(\eta^2\text{-}H_2SiPh_2)]$ (**1**) has an electronic structure intermediate between a Ti^{IV} silyl hydride and a Ti^{II} silane σ complex;[13] in other words, **1** is a stretched σ complex.[1a] In related work Harrod et al. extensively studied the reactions of dimethyl titanocene with silanes, which give either mononuclear Ti^{III} silyl or dimeric titanocene silyl hydrides with agostic Si-H-Ti interactions.[14] They also found that the reaction of $[Ti(Cp)_2(PMe_3)_2]$ with

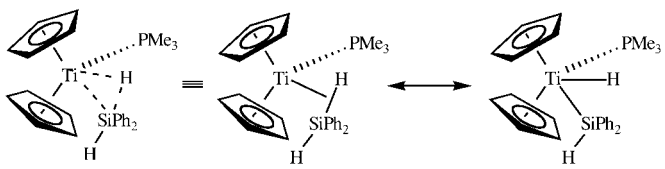

1

[a] Dr. G. I. Nikonov
Chemistry Department, Moscow State University
Vorob'evy Gory, 119992 Moscow (Russia)
Fax: (+7) 095-9328846
E-mail: nikonov@org.chem.msu.su

[b] Dr N. H. Rees, B. R. Tyrrell, Dr. S. R. Dubberley, Dr. P. Mountford
Department of Chemistry, University of Oxford
Chemistry Research Laboratory
Mansfield Road, Oxford OX1 3TA (UK)
Fax: (+44) 8165-272690
E-mail: philip.mountford@chem.ox.ac.uk

[c] Dr. S. K. Ignatov, Dr. A. G. Razuvaev
University of Nizhnii Novgorod
23, Gagarin Avenue, Nizhnii Novgorod 603600 (Russia)

 DOI: 10.1002/chem.200400230

$PhSiH_3$ gives a close analogue of **1**, namely, the silane σ complex $[Ti(Cp)_2(PMe_3)(\eta^2\text{-}H_3SiPh)]$.[15] A complex reported by Hartwig et al.[16] as $[Ti(Cp)_2(\eta^2\text{-}HBcat')(\eta^2\text{-}H_3SiPh)]$ (cat′ = catechol) was later suggested to be a silylborato complex $[Ti(Cp)_2(\eta^2\text{-}H_2Bcat')(SiH_2Ph)]$ on the basis of theoretical studies.[17] No fully authenticated, classical mononuclear silyl hydride complex of Ti^{IV} has been reported to date.

Intrigued by these earlier results, we recognized that the closely related, but previously unknown, chlorosilyl complexes $[Ti(Cp)_2(PMe_3)(H)(SiClRR')]$ (**2**) should be isolobal analogues of the Nb and Ta metallocene and metallocene-like compounds **3** and **4**, which exhibit M-H-Si-Cl IHIs.[6,7] Taken together, this hypothesis and the earlier studies of Buchwald et al., Harrod et al., and others posed important questions concerning 1) the nature of the Si–H interactions in complexes of types **1** and **2**, and 2) the accessibility of classical mononuclear titanocene silyl hydrides. We addressed these issues by a combination of synthetic, spectroscopic, X-ray diffraction, and DFT methods. We report here that the titanocene–phosphane ligand system is unique in that, depending on the nature of the silyl group substituents, different types of nonclassical bonding can be realized for the same Cp_2/PMe_3 environment, and that the classical Ti^{IV} silyl hydride form appears to be inaccessible.

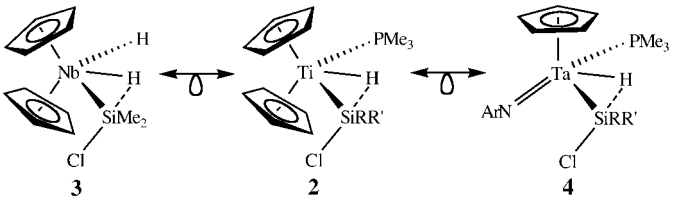

3 **2** **4**

Abstract in Russian:

Силилгидридные производные титаноцена, $[Ti(Cp)_2(PMe_3)(H)(SiR_3)]$ (SiR_3 = SiMePhCl (**6**), $SiPh_2Cl$ (**7**), $SiMeCl_2$ (**8**), $SiCl_3$ (**9**)), были получены по реакции окислительного присоединения силана $HSiR_3$ к $[Ti(Cp)_2(PMe_3)_2]$ и изучены методами ЯМР и ИК спектроскопии, РСА (для **6**, **8** и **9**) и расчетами методом функционала плотности (МФП). Результаты спектральных и структурных исследований показывают, что в этих силилгидридных комплексах титаноцена существуют неклассическое межлигандное гипервалентное взаимодействие Ti-H···Si-Cl. В часности, наблюдение константы спин-спинового взаимодействия кремний-гидрид *J*(Si-H) в **6**-**9** в диапазоне 22-40 Гц, знак которой, как мы показали, отрицателен для $[Ti(Cp)_2(PMe_3)(H)(SiCl_2Me)]$ и $[Ti(Cp)_2(PMe_3)(H)(SiCl_3)]$, является убедительным свидетельством присутствия прямой связи Si-H. Аналогичная реакция $[Ti(Cp)_2(PMe_3)_2]$ с $HSi(OEt)_3$ также не приводит к ожидаемому классическому силилгидриду $[Ti(Cp)_2(PMe_3)(H)\{Si(OEt)_3\}]$, вместо этого возникает продукт реакции перераспределения групп в силане, $Si(OEt)_4$, и титановый комплекс, невидимый в спектрах ЯМР (по-видимому, комплекс(ы) Ti^{III}). Структурные данные и результаты расчетов МФП соединений $[Ti(Cp)_2(PMe_3)(H)(SiR_3)]$ показывают, что сила межлигандных гипервалентных взаимодействий в хлорсилильных комплексах уменьшается по мере роста числа хлоридных заместителей при атоме кремния. Однако, при отсутствии электроакцепторной группы при кремнии, лежащей в *транс* – положении к гидриду Si···H, возникает σ-комплекс силана, охарактеризованный длинной связью Ti-Si (2.658 Å) и коротким контактом Si-H (1.840 Å) в модельном комплексе $[Ti(Cp)_2(PMe_3)(H)(SiMe_3)]$. И σ-комплекс силана, и силилгидридные комплексы с межлигандными гипервалентными взаимодействиями показывают связевые пути между атомами кремния и гидрида в исследовании ABM (Атом-в-Молекуле). К настоящему времени классические титаноценовые силилгидридные комплексы без *какого-либо* взаимодействия Si-H не были получены, а известные силилгидриды титаноцена являются, в зависимости от природы группы R при Si, либо σ-комплексом силана, либо соединением с межлигандным гипервалентным взаимодействием.

Results and Discussion

Preparation of titanocene silyl hydrides: Following the approach of Buchwald et al.,[13] $[Ti(Cp)_2(PMe_3)_2]$ was treated with a series of silanes to afford extremely air and moisture sensitive yellow silyl hydrido complexes **5**–**9** (scheme 1) in high yield.

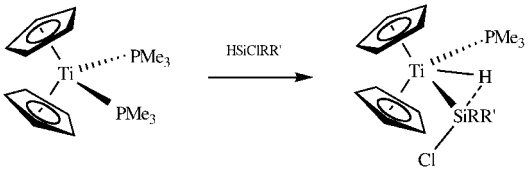

Scheme 1. Complex **5**: R = R′ = Me; complex **6**: R = Me, R′ = Ph; complex **7**: R = R′ = Ph; complex **8**: R = Me, R′ = Cl; complex **9**: R = R′ = Cl.

Complex **5**, obtained as a yellow powder, was too unstable in solution to allow NMR characterization. It decomposes slowly as a solid and rapidly in solution into the known blue compound $[Ti(Cp)_2(PMe_3)Cl]$, the identity of which was established by elemental analysis and an X-ray study.[18] The stability of **5**–**9** increases markedly with the number of chloro substituents on the silicon atom, so that in aromatic solvents at room temperature **6** is stable for about half an hour, **7** for a few hours, and **8** for several days, whereas **9** does not decompose over a period of several weeks. As a solid **9** does not show any sign of decomposition for at least several months.

The ^1H NMR spectra of **6**–**9** show well-defined signals attributed to Cp, PMe_3, and silyl ligands. As in **1**, the hydride resonances of **6**–**9** are found at about −4 ppm as doublets due to coupling to PMe_3 (Table 1). With the exception of **7**, the hydride resonance moves to lower field as the electronegativity of the substituents at silicon increases. This trend is consistent with the decreased hydridic character of the Ti–H hydrogen atom and also is in agreement with a decrease in the extent of IHI between the hydrogen and silicon atoms (vide infra) along this series.[6] Supporting this view is the increase in the magnitude of the values of $^2J(^1H,^{31}P)$ (Table 1), which are consistent with strengthening of the Ti–H interaction. The IR spectra of **6**–**9** display hydride-associated bands

Table 1. Selected spectroscopic data[a] for complexes $[Ti(Cp)_2(PMe_3)(H)(SiRR'Cl)]$ (**5**–**9**).

	5[b]	**6**	**7**	**8**	**9**
$\tilde{\nu}_{Ti-H}$ [cm^{-1}]	1611	1574	1566	1538	1524
δ^1H(TiH) [ppm]	–	−4.67	−3.92	−4.35	−3.61
^2J(P,H) [Hz]	–	74.7[c]	67.8[c]	82.8[c]	90.9[c]
J(Si,H) [Hz]	–	31[c]	40[c]	−22	−34

[a] NMR data in C_6D_6, IR data in Nujol. [b] NMR data for **5** are absent due to its extreme instability in solution. [c] Absolute values, sign not determined.

in the region 1524–1611 cm^{-1}. In mononuclear hydrides of titanium the Ti–H stretch typically shifts to lower frequency as the formal oxidation state of titanium changes from IV to III. Thus, in well-defined Ti^{IV} compounds the Ti–H band is observed in the range of 1532–1645 cm^{-1},[19] whereas in titanocene monohydrides $[Cp''_2TiH]$ (Cp'' = substituted cyclopentadienyl) this band is found in the range 1475–1505 cm^{-1}.[20] The hydride-associated stretch in **1**, which has an oxidation state intermediate between IV and II, is closer to the second range (1508 cm^{-1}).[13] The unexpected feature of **5**–**9** is that the Ti–H bands shift to lower frequency on going from **5** to **9** as the electronegativity of substituents at silicon increases. Electron-withdrawing groups at silicon are normally expected to promote a more extensive degree of oxidative addition of the Si–H bond to a metal center,[1a,c,d] and thus a more pronounced formal oxidation state of IV for Ti. Furthermore, this trend apparently contradicts the strengthening of the Ti–H interaction observed in DFT calculations (vide infra). However, this apparent contradiction is easily explained if one takes into account the occurrence of interligand interactions between the hydride and silyl groups in these compounds (vide infra). For this reason it is incorrect to interpret the IR data simply in terms of strengthening/weakening of independent Ti–H and/or Si–H bonds, as the Si–H and Ti–H vibrations are evidently correlated.

The magnitude of the silicon–hydride coupling constants J(Si,H) in **6**–**9** (31, 40, 22, and 34 Hz, respectively) are comparable to that in **1** (28 Hz)[13] and in the complexes $[Cp(ArN)Ta(PMe_3)(H)(SiMe_{3-n}Cl_n)]$ (n = 1–3, range 33–50 Hz) with IHIs.[7b] Although it has become conventional to infer the presence of nonclassical Si–H interactions on the basis of large Si–H coupling constants (> 20 Hz),[1a–d] recent studies have established that there is no strict correlation between the strength of the Si–H interaction and the magnitude of J(Si,H).[7b,21].

Since the scalar coupling constant is primarily a through-bond interaction the observed coupling constant can be thought of as the sum of one- (H–Si) and two-bond (H-M-Si) interactions [Eq. (1)].

$$J^{obs}(Si,H) = {}^1J(Si,H) + {}^2J(Si,H) \quad (1)$$

The relative signs and magnitudes of the two coupling constants will determine the magnitude and sign of the observed coupling constant. The one-bond coupling constant ^1J(Si,H) is known to be negative,[22] and in many cases two-bond coupling constants involving silicon are positive.[22] Because variation of the substituents at silicon can change the percentage of Si 3s and 3p orbitals participating in the Si–M and Si–H bonds,[7b,21b,23] they can, in theory, alter both the magnitude and the sign of the observed coupling constant. This might, in turn, result in an irregular change in the magnitude of the observable coupling constant $|J^{obs}(Si,H)|$ as the electronegativity of the substituents is varied. Another problem can arise if the magnitudes of ^1J(Si,H) and ^2J(Si,H) are comparable. In this case it is possible that a large negative value of ^1J(Si,H), indicative of the presence of a direct Si–H interaction, could be compensated by a large positive value of ^2J(Si,H). This might happen, for example, when an increase in the electronegativity of the substituents at silicon increases the two-bond component ^2J(Si,H) due to increased Si 3s character in the M–Si bond.[7b,21b,23] In this case a small value of $|J^{obs}(Si,H)|$ would be highly misleading if taken as the sole indicator of the absence of Si–H interactions. It appears that the sign of J^{obs}(Si,H) might at least provide an additional and meaningful indicator because, if negative, it at least shows the dominance of ^1J(Si,H) over ^2J(Si,H). We determined the signs of J(Si,H) in both **8** and **9**, and since both values are negative, this establishes the presence of a direct covalent interaction between the silicon and hydrogen atoms. Attempts to determine the sign of J(Si,H) in complexes **1**, **6**, and **7** were unsuccessful.

Below we present structural and theoretical evidence that **5**–**9** have nonclassical H–Si interactions. In the light of this and the nonclassical nature of **1**[13] it was of interest to try to synthesize a classical titanocene silyl hydride. The target compound should have substituents at silicon electronegative enough to promote complete oxidative addition of Si–H to a metal atom,[24] but these should not be electron-withdrawing and/or good leaving groups in order to avoid IHI.[6,7] Because alkoxyl groups have been shown to cause only weak (if any)[6c] IHI, we decided to study the reaction of $HSi(OEt)_3$ with $[Ti(Cp)_2(PMe_3)_2]$. In contrast to the facile formation of **1** and **5**–**9**, however, carrying out the reaction under the conditions used for other silanes does not result in the precipitation of a yellow compound. Two silicon-containing species were identified from the ^{29}Si NMR spectrum of the reaction mixture. One of them displays a signal at −59.1 ppm coupled to one hydrogen atom with J(Si,H) = 286 Hz; the second signal at −89.9 ppm is not proton-coupled. We assign these signals to unconsumed $HSi(OEt)_3$ (present in excess) and $Si(OEt)_4$,[25] respectively. Redistribution of the groups in $HSi(OEt)_3$ by a titanocene complex to give a SiH_3 ligand and $Si(OEt)_4$ was previously documented by Harrod et al.[14a] Monitoring the reaction by ^{1}H NMR spectroscopy did not show formation of any hydride complex with a Ti–H signal in the expected chemical shift region (> 0 ppm). However, the decrease in signals due to $HSi(OEt)_3$ and $[Ti(Cp)_2(PMe_3)_2]$ shows that some reaction does occur, apparently producing NMR-silent paramagnetic products. This result suggests that $[Ti(Cp)_2(PMe_3)(H)\{Si(OEt)_3\}]$ is not formed as a stable product and that the presence of interligand interactions (residual interactions as in σ complexes like **1** or with IHI as in **3** and **4**) is important in stabilizing the addition of silanes to the titanocene phosphane fragment $[Ti(Cp)_2(PMe_3)]$.

X-ray diffraction studies: The solid-state structures of **6**, **8**, and **9** were determined by X-ray diffraction, and the molecular structures are shown in Figure 1. Selected molecular parameters of **6**, **8**,and **9** can be found in Table 2, respectively. In accordance with Bent's rule,[23] the average Si–Cl bond length (2.223(2) Å in **6**, 2.163(1) Å in **8**, 2.125(1) Å in **9**) shortens as the number of chloro substituents increases.[6a] As is typical for complexes with IHI, one of the chlorine atoms in **6**, **8**, and **9** is located in the bisecting plane of the metallocene moiety *trans* to the hydride, which enables transfer of electron density from the M–H bond orbital to the (Si–Cl)* antibonding orbital of the Si–Cl bond.[6a] This results in elongation of the M–H and Si–Cl bonds and shortening of the M–Si and Si–H distances.[6,7] The Si–Cl(*trans*) bond of 2.223(2) Å in **6** is remarkably long, even much longer than in other complexes with IHI (2.163–2.177(2) Å).[6,7] Importantly, the Si–Cl(*trans*) bond in **8** and **9** is noticeably longer than the out-of-plane Si–Cl bonds ($\Delta = 0.059(2)$ and 0.055(2) Å, respectively), and even in **9** the difference is unusually large. In comparison, the two Si–Cl bonds in the isolobal complex $[Ta(Cp)(ArN)(PMe_3)(H)(SiMeCl_2)]$ with IHI are both shorter (2.117(2) and 2.064(3) Å) and have somewhat smaller Δ (0.053(4) Å) than the Si–Cl bonds in **8** (2.192(1) and 2.133(1) Å, $\Delta =$ 0.059(2) Å). The Si–Cl(*trans*) bond of 2.192(1) Å in **8** is significantly longer than the Si–Cl bonds in previously reported complexes of the type $[M(L)_nSiRCl_2]$ (2.007–2.130 Å),[26] for which longer distances are found for complexes with Si–Cl bonds elongated due to either nonclassical interactions between the silyl and hydride ligands[26b] or negative hyperconjugation between a metal-centered lone pair and the (Si–Cl)* antibonding orbital.[26h]

The hydride ligands of **8** and **9** were found in Fourier difference maps and refined to Ti–H distances of 1.73(2) and 1.72(2) Å, respectively. Titanium-to-terminal hydride bond lengths determined by X-ray diffraction span a wide range of 1.70(4)–1.96(6), possibly reflecting the experimental uncertainties associated with location of H atoms by this method.[20a,b,27,28] The Si–H(hydride) distances in **8** and **9** of 1.75(2) and 1.75(3) Å, respectively, are suggestive of the presence of significant Si–H interactions.[1] Although the M–H distances cannot be reliably established by X-ray diffraction due to systematic foreshortening, these short Si–H distances are not simply the result of long Ti–H bonds; rather they stem from small Si-Ti-H bond angles (Si-Ti-H in **8** is 44.0(6)° versus 64.5(6)° for H-Ti-P; in **9** the corresponding values are 44.6(8) and 64.3(8)°). This structural feature is further supported by DFT calculations (vide infra). Taken together these structural data suggest the presence of strong

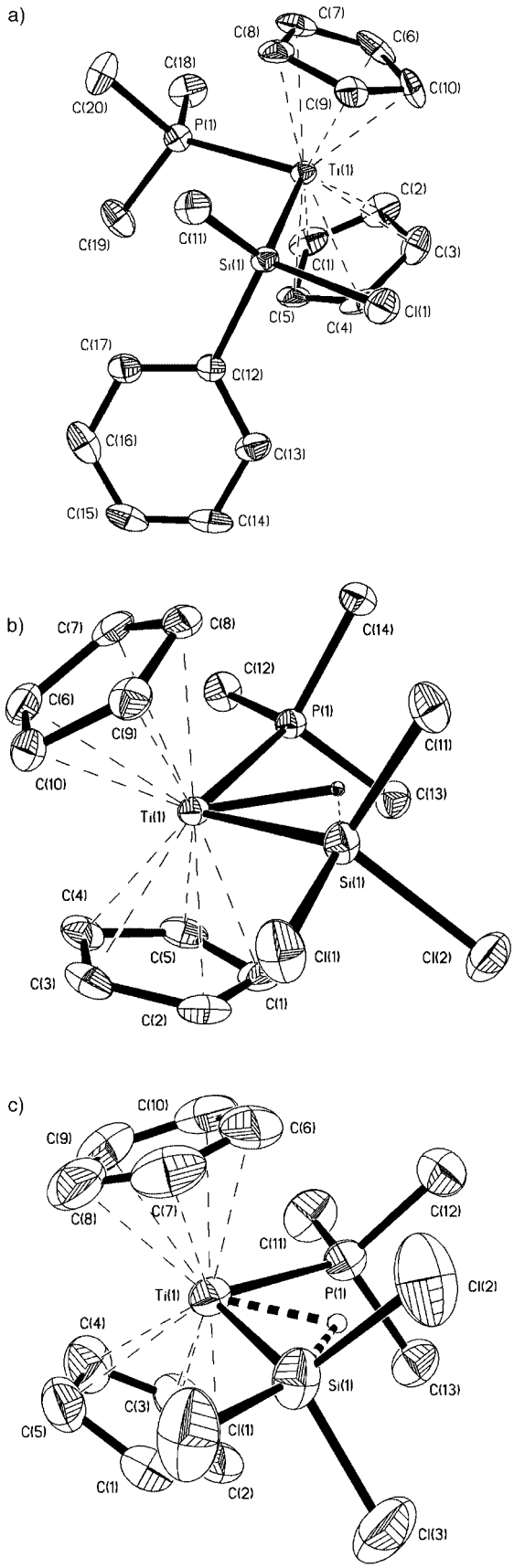

Figure 1. Top: Molecular structure of $[Ti(Cp)_2(PMe_3)(H)(SiClMePh)]$ (**6**). Displacement ellipsoids (non-H atoms) are shown at 50% probability. Hydrogen atoms are omitted for clarity. The hydride ligand was not found. Middle: Molecular structure of $[Ti(Cp)_2(PMe_3)(H)(SiCl_2Me)]$ (**8**). Displacement ellipsoids (non-H atoms) are shown at 50% probability. Hydrogen atoms are omitted for clarity. Bottom: Molecular structure of $[Ti(Cp)_2(PMe_3)(H)(SiCl_3)]$ (**9**). Displacement ellipsoids (non-H atoms) are shown at 50% probability. Hydrogen atoms (apart from hydride) are omitted for clarity.

Table 2. Selected bond lengths [Å] and angles [°] for $[Ti(Cp)_2(PMe_3)(H)(SiMePhCl)]$ (**6**), $[Ti(Cp)_2(PMe_3)(H)(SiMeCl_2)]$ (**8**), and $[Ti(Cp)_2(PMe_3)(H)(SiCl_3)]$ (**9**).

Compound **6**							
Ti(1)–Si(1)	2.545(2)	Ti(1)–P(1)	2.558(2)	Cl(1)–Si(1)	2.223(2)	Si(1)–C(11)	1.896(7)
Si(1)–C(12)	1.904(7)						
Si(1)-Ti(1)-P(1)	108.93(7)	Cl(1)-Si(1)-Ti(1)	114.80(9)	C(11)-Si(1)-C(12)	104.2(3)	C(11)-Si(1)-Cl(1)	97.7(2)
C(12)-Si(1)-Cl(1)	99.9(2)	C(11)-Si(1)-Ti(1)	119.8(2)	C(12)-Si(1)-Ti(1)	117.1(2)		
Compound **8**							
Ti(1)–Si(1)	2.5167(7)	Ti(1)–P(1)	2.5532(11)	Si(1)–Cl(1)	2.192(1)	Si(1)–Cl(2)	2.134(1)
Si(1)–C(11)	1.8853(16)	Ti(1)–H	1.733(18)	Si(1)–H	1.749(17)		
Si(1)-Ti(1)-P(1)	108.39(3)	Cl(1)-Si(1)-Cl(2)	100.78(6)	Cl(1)-Si(1)-Ti(1)	117.36(3)	Cl(2)-Si(1)-Ti(1)	116.30(3)
Cl(1)-Si(1)-C(11)	98.43(6)	Cl(2)-Si(1)-C(12)	97.46(4)	C(11)-Si(1)-Ti(1)	122.18(6)	Si(1)-Ti(1)-H	44.0(6)
P(1)-Ti(1)-H	64.5(6)						
Compound **9**							
Ti(1)–Si(1)	2.491(1)	Ti(1)–P(1)	2.5559(13)	Si(1)–Cl(1)	2.1606(14)	Si(1)–Cl(2)	2.1090(14)
Si(1)–Cl(3)	2.1036(12)	Ti(1)–H	1.72(2)	Si(1)–H	1.75(3)		
Si(1)-Ti(1)-P(1)	108.88(4)	Cl(1)-Si(1)-Ti(1)	120.18(4)	Cl(2)-Si(1)-Ti(1)	118.40(5)	Cl(3)-Si(1)-Ti(1)	118.25(5)
Cl(1)-Si(1)-Cl(2)	97.56(5)	Cl(1)-Si(1)-Cl(3)	98.03(5)	Cl(2)-Si(1)-Cl(3)	100.07(5)	Si(1)-Ti(1)-H	44.6(8)
P(1)-Ti(1)-H	64.3(8)						

nonclassical Si–H interactions in **6**, **8**, and **9**. The small size of the titanium atom contributes only marginally to the shortening of the Si–H distances. Thus, the distances from the silicon atom to the midpoint of the Si–P vectors (the likely hydride location if the structure were classical) in **8** and **9** are much longer (2.053 and 2.056 Å, respectively). Therefore, placing the hydride ligand in the central position in the titanocene bisecting plane would have resulted in a significantly longer Si–H distances. In conclusion, the structural features of **6**, **8**, and **9** suggest the presence of nonclassical interligand interactions which must have an electronic origin.

DFT calculations: To elucidate the bonding situation in **1** and **5–9**, a series of model complexes $[Ti(Cp)_2(PMe_3)(H)(SiMe_{3-n}Cl_n)]$ [$n=0$ (**10**), 1 (**11**), 2 (**12**), 3 (**13**)] were calculated with the DFT method. The calculated structures **12** and **13** are exact models of the real compounds **8** and **9**, respectively. There is a very good agreement between the calculated and observed values and trends (Table 3). In particular, the shortening and strengthening of the Ti–Si bond along the series is nicely seen [expressed by large Wiberg bond indices[29] (WI; Table 4), NBO bond orders[30] (Table 5) and negative $H(\boldsymbol{r}_c)$ values (Table 6) in an Atoms in Molecules (AIM) study[31]], as is the longer and weaker Si–Cl bond *trans* to the hydride compared to the out-of-plane Si–Cl bond. These trends indicate the presence of IHI in **11–13**.[6,7] The Si–H contacts in **10–13** are very short and have remarkably large WI, a manifestation of nonclassical structures. Furthermore, the AIM study found bond critical points[31] for the Si–H bonds in all compounds. Apart from the Ti–Si bond length, other parameters in **11–13** do not change monotonically along the series. The Si–H bond length in the series **10–13** has a minimum for **11**, decreasing from **10** to **11** and **12** and elongating as the number of chloro substituents in the silyl groups increases, while the Ti–H bond length also changes irregularly and has a maximum for **11**. The data given in Tables 3, 4, 5and 6 show that the weakening of

Table 3. Selected calculated bond lengths [Å] for $[Ti(Cp)_2(PMe_3)(H)(SiMe_{3-n}Cl_n)]$ ($n=0$–3; **10–13**, respectively) and **14**.[a,b]

	10[c]	**11**[d]	**12**[e]	**13**[f]	**14**[a]
Ti–Si	2.658	2.581	2.535	2.520	
	(2.597)	(2.545)	(2.517)	(2.492)	
Ti–P	2.541	2.555	2.559	2.557	2.557
	(2.550)	(2.558)	(2.554)	(2.556)	
Ti–H	1.742	1.759	1.755	1.754	1.745
	(1.81)	(1.733)	(1.751)		
Si–H	1.840	1.805	1.822	1.847	1.862
	(1.69)		(1.749)	(1.751)	
Si–Cl	–	2.292[g]	2.259[g]	2.225[g]	–
		(2.223)	(2.192)	(2.161)	
	–	–	2.216[h]	2.190[h]	–2.218[h]
			(2.133)	(av 2.107)	

[a] **14** is a rotamer of **12** with the Me group *trans* to the hydride. [b] X-ray data in parentheses for comparison; in **8** and **9** the hydride ligands were located in the difference map and refined. [c] X-ray data for **1**. [d] X-ray data for **6**. [e] X-ray data for **8**. [f] X-ray data for **9**. [g] Cl *trans* to hydride. [h] Out-of-plane Cl.

Table 4. Selected Wiberg bond indices (WI) of $[Ti(Cp)_2(PMe_3)(H)(SiMe_nCl_{3-n})]$ ($n=0$–3; **10–13**, respectively) and **14**.[a]

	10	**11**	**12**	**13**	**14**
Ti–Si	0.4915	0.5948	0.6308	0.6578	0.6012
Ti–P	0.6822	0.6702	0.6698	0.6715	0.6746
Ti–H	0.4995	0.4957	0.5080	0.5186	0.5146
Si–H	0.3210	0.3188	0.2962	0.2729	0.2815
Si–Cl	–	0.6638[b]	0.7048[b]	0.7484[b]	–
	–	–	0.7617[c]	0.7930[c]	0.7583
$Si–C_{Me}$	0.7117[d]	–	–	–	0.7127
	0.7340[e]	0.7363	0.7375	–	–

[a] **14** is a rotamer of **12** with the Me group *trans* to the hydride. [b] Cl trans to hydride. [c] Out-of-plane Cl. [d] Me *trans* to hydride. [e] Out-of-plane Me.

Table 5. Selected atom–atom overlap-weighted NAO bond orders of $[Ti(Cp)_2(PMe_3)(SiMe_nCl_{3-n})(H)]$ ($n=0$–3).

	$SiCl_3$	$SiMeCl_2$	$SiMe_2Cl$	$SiMe_3$	$SiMeCl_2$[a]
Ti–Si	0.5650	0.5372	0.5033	0.4333	0.5230
Ti–P	0.5232	0.5265	0.5336	0.5512	0.5317
Ti–H*	0.4113	0.4079	0.4049	0.4112	0.4114
Si–H*	0.3828	0.4018	0.4189	0.4146	0.3886
Si–Cl (ip[b])	0.6370	0.6081	0.5801	–	–
Si–Cl (oop[c])	0.6609	0.6401	–	–	0.6389
$Si–C_{Me}$ (ip)	–	–	–	0.7125	0.7393
$Si–C_{Me}$ (oop)	–	−0.7460	−0.7366	–	0.7273

[a] A rotamer of **12** with the Me group *trans* to hydride. [b] ip = in-plane. [c] oop = out-of-plane.

Table 6. Topological analysis of the electron density in $[Ti(Cp)_2(PMe_3)(H)(X)]$ at the BP86 level of theory.[a]

X	Bond[b]	$\rho(r_c)$ [e Å^{-3}]	$\nabla^2\rho(r_c)$ [e Å^{-3}]	ε_c	$H(r_c)$ [Hartree Å^{-3}]
$SiCl_3$	Ti–Si	0.4125	0.4025	0.4045	−0.1546
	Ti–P	0.3675	2.0562	0.4621	−0.1000
	Ti–H*	0.5450	2.8600	0.1807	−0.2000
	Si–H*	0.4942	−1.2335	0.2622	−0.2122
	Si–Cl(ip)	0.5296	−0.6835	0.0624	−0.3246
	Si–Cl(oop)	0.5539	−0.0050	0.0291	−0.3500
$SiMeCl_2$	Ti–Si	0.4185	0.1357	0.4623	−0.1574
	Ti–P	0.3607	2.1765	0.5131	−0.0947
	Ti–H*	0.5379	3.0443	0.2364	−0.1921
	Si–H*	0.5016	−1.4124	0.2717	−0.2311
	Si–Cl(ip)	0.4882	−0.5495	0.0968	−0.2850
	Si–Cl(oop)	0.5160	0.1414	0.0679	−0.3135
	$Si–C_{Me}$(oop)	0.7735	4.7159	0.0151	−0.4683
$SiMe_2Cl$	Ti–Si	0.3993	0.0800	0.6761	−0.1400
	Ti–P	0.3572	2.3290	0.5873	−0.0910
	Ti–H*	0.5278	3.1548	0.2789	−0.1841
	Si–H*	0.4969	−1.4805	0.2557	−0.2430
	Si–Cl(ip)	0.4481	−0.3321	0.0682	−0.2486
	$Si–C_{Me}$(oop)	0.7446	5.0631	0.0296	−0.4296
Si(*trans*-Me)Cl_2	Ti–Si	0.4091	0.1924	0.4040	−0.1505
	Ti–P	0.3627	2.1896	0.6266	−0.0962
	Ti–H*	0.5543	2.7821	0.1772	−0.2077
	Si–H*	0.4874	−1.1594	0.2716	−0.2000
	$Si–C_{Me}$(ip)	0.7586	4.2346	0.0218	−0.4612
	Si–Cl(oop)	0.5149	0.1594	0.0665	−0.3128
$SiMe_3$	Ti–Si	0.3621	0.3636	1.9239	−0.1063
	Ti–P	0.3609	2.5424	0.8466	−0.0908
	Ti–H*	0.5501	2.9126	0.2395	−0.2028
	Si–H*	0.4740	−1.3908	0.2229	−0.2160
	$Si–C_{Me}$(ip)	0.6936	4.5723	0.0310	−0.3844
	$Si–C_{Me}$(oop)	0.7179	5.4362	0.0227	−0.3940

[a] $\rho(r_c)$ = electron density at the bond critical points, $\rho^2(r_c)$ = Laplacian of electron density at the bond critical points, $H(r_c)$ = sum of Hamiltonian kinetic energy density and potential energy density, ε_c = ellipticity. [b] ip = in-plane, oop = out-of-plane.

the Si–H bonds is accompanied by strengthening of the Ti–H bonds from **11** to **13**. Analogous trends have been previously observed for the isolobal complexes $[Ta(Cp)(ArN)(PMe_3)(H)(SiMe_{3-n}Cl_n)]$ ($n=1$–3) with IHI.[7b] In contrast, the conventional theory of σ-bond complexation predicts that increasing electronegativity of the substituents at the silicon atom should lead to a monotonic advance of the oxidative adition of the Si–H bond to the metal.[1a–d] Together these data suggest that the nature of the Si–H bonding in **10** and **11**–**13** is different. Specifically, the former is a silane σ complex with a weak Ti–Si bond, whereas **11**–**13** are chlorosilyl compounds with IHI of the type Ti-H-Si-Cl, which weakens for the more chlorinated silyl groups, behavior previously found for complexes **4**.[7b] Also in accordance with the latter description, the Laplacian at the Ti–H bond critical point r_c in **10**–**13** has large positive values (local electron density depletion), and the electron density at r_c exhibits a minimum for **11**, whereas for the Si–Cl (in-plane) bond $\nabla^2\rho(r_c)$ is negative (local electron density concentration). Taking into account that the Si–Cl (out-of-plane) bonds have positive Laplacians, this can be interpreted as a transfer of electron density from the Ti–H bonds onto the (Si–Cl)* (in-plane) antibonding orbital. Confirming a decrease in IHI, $H(r_c)$[31] for the Si–Cl (in-plane) bond decreases from **11** to **13**. Finally, the unique feature of **10** is that it has an increased ellipticity of the Ti–Si bond ($\varepsilon_c=1.9239$)[32] in accord with its description as a silane σ complex. Analysis of the Laplacian contour map of **10** shows that the Ti–Si bond critical point is close in magnitude to the ring critical point (0.3600 and 0.3621 e Å^{-3}, respectively), that is, a situation emerges where the Ti–Si bond is about to vanish, which means that the observed topological structure of $[Ti(Cp)_2(PMe_3)(\eta^2\text{-H-SiMe}_3)]$ is very close to that of $[Ti(Cp)_2(PMe_3)(\eta^1\text{-HSiMe}_3)]$. By way of contrast, for the other compounds **11**–**13** ε_c is in the range 0.4040–0.6761 and the ring critical points (0.3993–0.4185 e Å^{-3}) are located well away from the bond critical points (Table 6,) indicating stable topological structures, which allow us to can rationalize them in terms of silyl complexes (although still nonclassical silyl complexes).

In principle, increased electronegativity of the substituents at Si should promote the breaking of the Si–H interaction in a silane σ complex.[1] In an attempt to model a classical titanocene silyl hydride without IHI or residual Si–H σ bonding, we optimized rotamer **14** of $[Ti(Cp)_2(PMe_3)(H)(SiMeCl_2)]$, restricted to have the Me group *trans* to the hydride. As expected, **14** does have a much shorter and stronger Ti–Si bond than **10**, but although the Si–H distance of 1.862 Å is longer than in **10**, it is still well within bonding range,[1] and a bond critical point was found. Comparing **14** with **12** bearing the same silyl group ($SiMeCl_2$), one can see that in **14** both the Ti–Si bond and the Si–H interaction are longer and weaker, whereas the Ti–H bond is shorter and stronger. The two out-of-plane Si–Cl bonds in **14** are comparable in lengths and strength to the out-of-plane Si–Cl bond in **12**. Therefore, **14** is nonclassical but does not exhibit IHI, and it can be better described as a stretched silane σ complex. This result and our failure to prepare $[Ti(Cp)_2(PMe_3)(H)(Si(OEt_3)]$ (vide supra) compel us conclude that classical titanocene silyl hydrides (Ti^{IV} compounds) are unlikely to exist, regardless of the nature of the R group on Si. However, the type of Si–H interaction in nonclassical complexes $[Ti(Cp)_2(PMe_3)(H)(SiR_3)]$ does depend on R: they are σ complexes for electropositive R groups, and compounds with IHI if at least one electronegative group on Si is *trans* to the Si–H moiety.

Conclusion

Reactions of $[Ti(Cp)_2(PMe_3)_2]$ with silanes afford only nonclassical titanocene silyl hydrides; classical mononuclear titanocene silyl hydride continue to be elusive species. Unless stabilized by IHI, this system tries to escape the unfavorable oxidation state IV of titanium by forming either products of incomplete oxidative addition (stretched σ complexes with an oxidation state between II and IV) or paramagnetic Ti^{III} complexes. Spectroscopic and structural features of $[Ti(Cp)_2(PMe_3)(H_2SiPh_2)]$ (**1**), supported by a DFT study on a model complex, establish that this compound is a silane σ complex. The bonding situation in the isolated chlorosilyl derivatives is very different: these complexes exhibit Ti-H-Si-Cl interligand hypervalent interactions. Therefore, the titanocene fragment $[Ti(Cp)_2(PMe_3)]$ is unique in supporting two different types of nonclassical Si–H interaction.

Experimental Section

All manipulations were carried out by using conventional Schlenk techniques. Solvents were dried over sodium or sodium benzophenone ketyl and distilled into the reaction vessel by high-vacuum gas-phase transfer. NMR spectra were recorded on a Varian Mercury-*vx* (^{1}H, 300 MHz; ^{13}C, 75.4 MHz) and Unity-plus (^{1}H, 500 MHz; ^{13}C, 125.7 MHz) spectrometers. IR spectra were obtained as Nujol mulls with a FTIR Perkin-Elmer 1600 series spectrometer. $[Ti(Cp)_2Cl_2]$ and silanes were obtained from Sigma-Aldrich. $[Ti(Cp)_2(PMe_3)_2]$ was prepared according to the literature method. J(Si,H) coupling constants were measured from the ^{29}Si,^{1}H satellites in the ^{1}H NMR spectra. In **8** and **9** the sign of J(Si,H) was determined from a spin-tickling experiment in which the ^{1}H NMR spectrum of the titanium hydride was observed, while low-power continuous irradiation was applied sequentially at the positions of the low- and high-frequency ^{29}Si satellites of the proton-coupled ^{31}P resonance of the PMe_3 group; this resulted in sequential splitting of the low- and high-frequency ^{29}Si satellites in the ^{1}H spectrum. Therefore, in both **8** and **9** the sign of J(Si,H) is the same as that of ^2J(Si,P). The sign of ^2J(Si,P) is negative and was determined in the analogous complex $[Cp(ArN)Ta(PMe_3)(H)(SiMePhH)]$ by comparison to the negative sign of J(H,Si) which we reported previously.[7b]

Reaction of $[TiCp_2(PMe_3)_2]$ with $HSiMe_2Cl$: $HSiMe_2Cl$ (1.5 mL) was added to a solution of $[Ti(Cp)_2(PMe_3)_2]$ (1.60 g, 5.96 mmol) in pentane (80 mL). Immediate precipitation of a yellow powder occurred. The solution was quickly filtered and the residue was washed with pentane (7 mL) and dried in vacuo. Yield: 1.44 g (83 %). Attempts to prepare NMR samples of the product in a nitrogen-filled glove box resulted in decomposition. The compound gives rise to intensive blue color on dissolving in aromatic or ethereal solvents under argon or nitrogen. The ^{1}H NMR spectrum in C_6D_6 prepared under argon showed no signals in the regions typical for the Cp, PMe_3, and $SiMe_2$ groups. Keeping this material under argon or vacuum as a solid also results in the development of a blue color. Blue X-ray quality crystals were grown on cooling a solution of the product in diethyl ether. An X-ray study showed this to be the known compound $[Ti(Cp)_2(Cl)(PMe_3)]$. IR (Nujol): $\tilde{\nu}_{Ti-H} = 1611\ cm^{-1}$.

$[Ti(Cp)_2(PMe_3)(H)(SiClMePh)]$ (6): HSiClMePh (0.17 mL, 1.13 mmol) was added by syringe to solution of $[Ti(Cp)_2(PMe_3)_2]$ (0.276 g, 0.836 mmol) in diethyl ether (50 mL) at room temperature. Over 5 min the resultant brown solution was cooled to −30 °C, kept at this temperature for 2 d, and then slowly concentrated to 30 mL to produce yellow crystals. A second crop was obtained by further concentrating the solution to 4 mL and keeping it at −30 °C. Total yield: 0.134 g (0.326 mmol, 39 %). IR (Nujol): $\tilde{\nu}_{Ti-H} = 1574\ cm^{-1}$; ^{1}H NMR (300 MHz, C_6D_6, 25 °C): $\delta = 8.12$ (d, $J = 7.3$ Hz, 2H; *o*-Ph), 7.31 (t, $J = 7.3$ Hz, 2H; *m*-Ph, 7.19 (t, $J = 7.4$ Hz, 1H; *p*-Ph), 4.92 (d, J(P,H) = 2.5 Hz, 5H; Cp), 4.66 (d, J(P,H) = 2.4 Hz, 5H; Cp), 1.00 (s, 3H; SiMe), 0.61 (d, J(P,H) = 6.4 Hz, 9H; PMe), −4.67 ppm (d + dd, J(P,H) = 74.7 Hz, J(Si,H) = 31 Hz, 1H; TiH); ^{31}P NMR (121 MHz, C_6D_6, 25 °C): $\delta = 20.5$ ppm; elemental analyis calcd (%) for $C_{20}H_{28}NTiClPSi$ (410.83): C 58.47, H 6.68; dound: C 57.97, H 6.72. The ^{13}C NMR spectrum was not recorded because of rapid decomposition of the compound in solution. At room temperature **6** is stable for a half an hour in solution and for a day as a solid. X-ray quality crystals was obtained by cooling a solution of $[Ti(Cp)_2(PMe_3)(H)(SiClMePh)]$ in diethyl ether/toluene (1:1) to −30 °C.

$[Ti(Cp)_2(PMe_3)(H)(SiPh_2Cl)]$ (7): a) $HSiClPh_2$ (0.25 mL, 1.278 mmol) was added by syringe to a solution of $[Ti(Cp)_2(PMe_3)_2]$ (0.422 g, 1.278 mmol) in diethyl ether (20 mL), resulting in crystallization of yellow crystals, which were collected by filtration and dried in vacuo. Yield: 0.094 g (0.200 mmol, 16 %).

b) $HSiClPh_2$ (0.17 mL, 0.89 mmol) was added by syringe to a solution of $[Ti(Cp)_2(PMe_3)_2]$ (0.294 g, 0.89 mmol) in toluene (10 mL), resulting in crystallization of yellow crystals and formation of a purple solution. The crystals were collected by filtration and dried in vacuo. Yield: 0.260 g (0.511 mmol, 54 %).

IR (Nujol): $\tilde{\nu}_{Ti-H} = 1566\ cm^{-1}$; ^{1}H NMR (300 MHz, C_6D_6, 25 °C): $\delta = 8.33$ (d, $J = 7.8$ Hz, 4H; *o*-Ph), 7.26 (m, $J = 7.4$ Hz, 4H; *p*-Ph), 7.09 (m, 2H; *p*-Ph), 4.77 (d, J(P,H) = 2.4 Hz, 10H; Cp), 0.74 (d, J(P,H) = 9.3 Hz, 9H; PMe), −3.92 ppm (d + dd, J(P,H) = 67.8 Hz, J(Si,H) = 40.4 Hz, 1H; TiH); ^{13}C NMR (75 MHz, C_6D_6, 25 °C): $\delta = 148.0$ (*i*-Ph), 134.7 (*o*-Ph), 128.5 (*p*-Ph), 127.4 (*m*-Ph), 96.9 (Cp), 19.6 ppm (d, J(P,C) = 17.9 Hz, PMe); ^{31}P NMR (121 MHz, C_6D_6, 25 °C): $\delta = 19.8$ ppm; elemental analyis calcd (%) for $C_{25}H_{30}NTiClPSi$ (472.894): C 63.50, H 6.39; found: C 60.32, H 6.10. At room temperature **7** is stable in solution for several hours and as a solid for several days.

$[Ti(Cp)_2(PMe_3)(H)(SiCl_2Me)]$ (8): a) $HSiCl_2Me$ (0.4 mL, 3.84 mmol) was added by syringe to a solution of $[Ti(Cp)_2(PMe_3)_2]$ (0.178 g, 0.54 mmol) in pentane (10 mL), giving a yellow precipitate. This was collected by filtration, washed with pentane (2 mL) and dried. Yield: 0.10 g (0.271 mmol, 50 %).

b) $HSiCl_2Me$ (0.2 mL, 1.92 mmol) was added by syringe to a solution of $[Ti(Cp)_2(PMe_3)_2]$ (0.315 g, 0.954 mmol) in diethyl ether (30 mL). The color changed over a few minutes from dark brown to blue. After 5 min a yellow complex started to crystallize on the walls. The solution was cooled to −30 °C for 2 d, affording yellow crystals. These were collected by filtration, washed with pentane (2 mL), and dried. Yield: 0.138 g (0.374 mmol, 39 %).

IR (Nujol): $\tilde{\nu}_{Ti-H} = 1538\ cm^{-1}$; ^{1}H NMR (300 MHz, C_6D_6, 25 °C): $\delta = 4.84$ (br s, 10H; Cp), 1.24 (s, 3H; $SiMeCl_2$), 0.54 (d, J(P,H) = 6.6 Hz, 9H; PMe), −4.35 ppm (d + dd, J(P,H) = 82.8 Hz, J(Si,H) = 22 Hz, 1H; TiH); ^{13}C NMR (75 MHz, C_6D_6, 25 °C): $\delta = 96.7$ (Cp), 19.8 (d, J(P,C) = 19.2 Hz, PMe), 18.8 ppm (SiMe); ^{31}P NMR (121 MHz, C_6D_6, 25 °C): $\delta = 19.8$ ppm; elemental analyis calcd (%) for $C_{14}H_{23}NTiCl_2PSi$ (369.18): C 45.55, H 6.28; found: C 45.49, H 6.69. Compound **8** is stable in solution for days and as a solid for weeks.

$[Ti(Cp)_2(PMe_3)(H)(SiCl_3)]$ (9): $HSiCl_3$ (0.077 g, 0.566 mmol) was added by syringe to a solution of $[Ti(Cp)_2(PMe_3)_2]$ (0.187 g, 0.556 mmol) in pentane (10 mL). A yellow precipitate was immediately formed. This was collected by filtration, washed with pentane (2 mL), and dried. Yield: 0.17 g (0.436 mmol, 77 %). X-ray quality crystals were obtained by cooling a solution of **9** in diethyl ether to −30 °C for several days.

IR (Nujol): $\tilde{\nu}_{Ti-H} = 1524\ cm^{-1}$; ^{1}H NMR (300 MHz, C_6D_6, 25 °C): $\delta = 4.86$ (d, J(P,H) = 2.4 Hz, 10H; Cp), 0.54 (d, J(P,H) = 7.2 Hz, 9H; PMe_3), −3.61 ppm (d + dd, J(P,H) = 90.9 Hz, J(Si,H) = 34 Hz, 1H; TiH); ^{13}C NMR (75 MHz, C_6D_6, 25 °C): $\delta = 97.6$ (Cp), 20.0 ppm (d, J(P,C) = 21 Hz, PMe); ^{31}P NMR (121 MHz, C_6D_6, 25 °C): $\delta = 20$ ppm; elemental analyis calcd (%) for $C_{13}H_{20}NTiCl_3PSi$ (389.60): C 40.08, H 5.17; Found: C 40.77, H 5.07. Compound **9** is stable in solution for weeks and indefinitely as a solid under nitrogen or argon.

Reaction of $[Ti(Cp)_2(PMe_3)_2]$ with $HSi(OEt)_3$: An excess of $HSi(OEt)_3$ (ca. 4 equiv) was added to an NMR sample of $[Ti(Cp)_2(PMe_3)_2]$ in C_6D_6. Monitoring of the reaction over several days showed no formation of new Cp- and/or hydride-containing compounds. The declining signals due to $[Ti(Cp)_2(PMe_3)_2]$ and two sets of signals due to the Et group were observed. The ^{29}Si NMR spectrum of the reaction mixture showed presence of two silicon species, with signals at −59.1 ppm (coupled to hydrogen with J(Si,H) = 286 Hz) and −89.9 ppm (not coupled to hydrogen).

X-ray structure analyses: For all compounds the crystals were mounted in a film of perfluoropolyether oil on a glass fiber and transferred to a Siemens three-circle diffractometer with a CCD detector (SMART system). For all structures the data were corrected for Lorentzian and polarization effects. The structures were solved by direct methods[33] and refined by full-matrix least-squares procedures.[34] All non-hydrogen atoms were refined anisotropically. The hydride atoms were located from Fourier difference synthesis and positionally refined isotropically; all other hydrogen atoms were placed in calculated positions and refined in a riding model.

Compound 6: An X-ray quality crystal was obtained by cooling a solution of **6** in diethyl ether/toluene (1/1) to −30 °C. The yellow block with dimensions 0.10×0.10×0.20 mm was covered with oil and mounted at 150(2) K. Crystal data: $C_{20}H_{28}ClPSiTi$, M_r=410.83, hexagonal, space group $P6_1$, a=9.251(1), b=9.251(1), c=41.770(8) Å, α=90, β=90, γ=120°, V=3095.9(9) Å^3, Z=6, ρ_{calcd}=1.322 g cm^{-3}. Data collection: Θ range 2.93–27.49°, *hkl* ranges −12 to 12, −9 to 9, −52 to 54, 4052 measured reflections, 2824 of which were unique, μ=0.679 mm^{-1}. R=0.050, R_w=0.108 (observed reflections), and $R1$=0.099, $wR2$=0.168 (all data), 221 parameters, GOF=1.066. The largest peak in the final difference Fourier map had an electron density of 0.792 e Å^{-3}, and the lowest hole −0.788 e Å^{-3}. The location and magnitude of the residual electron density were of no chemical significance.

Compound 8: X-ray quality crystals of **8** were grown from a saturated solution in diethyl ether/hexane by cooling to −30 °C. A yellow block with dimensions 0.22×0.22×0.34 mm was covered with oil and mounted at 150(2) K. Crystal data: $C_{14}H_{23}Cl_2PSiTi$, M_r=369.18, triclinic, space group $P\bar{1}$, a=8.211(2), b=8.831(2), c=12.942(3) Å, α=83.28(3), β=88.28(3), γ=64.61(3)°, V=841.7(3) Å^3, Z=2, ρ_{calcd}=1.457 g cm^{-3}. Data collection: Θ range 5.14–27.56°, *hkl* ranges −10 to 10, −11 to 11, −16 to 16, 3819 measured reflections, of which 3469 were unique, μ=0.977 mm^{-1}. R=0.026, R_w=0.064 (observed reflections), and $R1$=0.030, $wR2$=0.062 (all data), 264 parameters, GOF=1.051. The largest peak in the final difference Fourier map had an electron density of 0.324 e Å^{-3}, and the lowest hole −0.340 e Å^{-3}. The location and magnitude of the residual electron density were of no chemical significance.

Compound 9: An X-ray quality crystal was obtained by cooling a solution of **9** in diethyl ether to −30 C for several days. The yellow plate with dimensions 0.10×0.60×0.60 mm was covered with oil and mounted at 150(2) K. Crystal data: $C_{13}H_{20}Cl_3PSiTi$, M_r=389.60, triclinic, space group $P\bar{1}$, a=8.303(2), b=8.860(2), c=12.988(3) Å, α=83.51(3), β=88.57(3), γ=64.70(3)°, V=858.0(3) Å^3, Z=2, ρ_{calcd}=1.508 g cm^{-3}. Data collection: Θ range 5.12–27.48°, *hkl* ranges −10 to 9, −11 to 11, −16 to 16, 3853 measured reflections, of which 2809 were unique, μ=0.977 mm^{-1}. $R1$=0.040, $wR2$=0.073 (observed reflections), and $R1$=0.069, $wR2$=0.083 (all data), 252 parameters, GOF=1.017. The largest peak in the final difference Fourier map had an electron density of 0.558 e Å^{-3}, and the lowest hole −0.445 e Å^{-3}. The location and magnitude of the residual electron density were of no chemical significance.

CCDC-211915 (**6**), CCDC-211916 (**8**) and CCDC-211917 (**9**) contain the supplementary crystallographic data for this paper. These data can be obtained free of charge via www.ccdc.cam.ac.uk/conts/retrieving.html (or from the Cambridge Crystallographic Data Centre, 12 Union Road, Cambridge CB21EZ, UK; fax: (+44) 1223-336-033; or deposit@ccdc.cam.uk).

DFT calculations: All calculations were carried out with the Gaussian 98 program package (Revision A.3) using DFT with Becke's 1988 nonlocal exchange functional in conjunction with Perdew's correlation functional (BP86).[35] The compound basis set used for the calculation consisted of the 6-31G(d) basis set for the Si, P, and N atoms, the 6-31G basis set for the carbon atoms and the silyl hydrogen atoms, and the 3-21G basis set for the H atoms of Cp rings and Me groups. The basis set augmented by the p-polarization function (6-31G(d,p) basis set) was used for the hydride H atom. The Hay–Wadt effective core potentials (ECP) and the corresponding VDZ basis sets were used for the titanium atom,[36] and the Stuttgart quasirelativistic ECP[37] was used for the Cl atom in this model. For more details and references, see reference [7a].

Acknowledgement

This work was supported through a Royal Society (London) joint research grant to G.I.N. and P.M., a YS INTAS fellowship to G.I.N., a RFBR grant (project 03–03–33120) to S.K.I. and A.G.R., and by EPSRC awards to B.R.T. and S.R.D.

[1] a) G. J. Kubas, *Metal Dihydrogen and σ-Bond Complexes*, Kluwer Academic/Plenum, New York, **2001**; b) R. H. Crabtree, *Angew. Chem.* **1993**, *105*, 828; *Angew. Chem. Int. Ed. Engl.* **1993**, *32*, 789; c) U. Schubert, *Adv. Organomet. Chem.* **1990**, *30*, 151; d) J. Y. Corey, J. Braddock-Wilking, *Chem. Rev.* **1999**, *99*, 175; e) Z. Lin, *Chem. Soc. Rev.* **2002**, *31*, 239; f) G. I. Nikonov, *J. Organomet. Chem.* **2001**, *635*, 24.

[2] a) W. A. Herrmann, N. W. Huber, J. Behm, *Chem. Ber.* **1992**, *125*, 1405; b) L. J. Procopio, P. J. Carroll, D. H. Berry, *J. Am. Chem. Soc.* **1994**, *116*, 177; c) W. A. Herrmann, J. Eppinger, M. Spiegler, O. Runte, R. Anwander, *Organometallics* **1997**, *16*, 1813; d) I. Nagl, W. Scherer, M. Tafipolsky, R. Anwander, *Eur. J. Inorg. Chem.* **1999**, 1405; e) J. Eppinger, M. Spiegler, W. Hieringer, W. A. Herrmann, R. Anwander, *J. Am. Chem. Soc.* **2000**, *122*, 3080; f) M. G. Klimpel, H. W. Görlitzer, M. Tafipolsky, M. Spiegler, W. Scherer, R. Anwander, *J. Organomet. Chem.* **2002**, *647*, 236; g) G. I. Nikonov, P. Mountford, J. C. Green, P. A. Cooke, M. A. Leech, A. J. Blake, J. A. K. Howard, D. A. Lemenovskii, *Eur. J. Inorg. Chem.* **2000**, 1917; h) S. K. Ignatov, N. H. Rees, S. R. Dubberley, A. G. Razuvaev, P. Mountford, G. I. Nikonov, *Chem. Commun.* **2004**, 952.

[3] a) N. Peulecke, A. Ohff, P. Kosse, A. Tillack, A. Spannenberg, R. Kempe, W. Baumann, V. V. Burlakov, U. Rosenthal, *Chem. Eur. J.* **1998**, *4*, 1852; b) M.-F. Fan, Z. Lin, *Organometallics* **1997**, *16*, 494; c) U. Schubert, M. Schwartz, F. Möller, *Organometallics* **1994**, *13*, 1554; d) J. Yin, J. Klozin, K. Abboud, W. M. Jones, *J. Am. Chem. Soc.* **1995**, *117*, 3298; e) U. Schubert, H. Giges, *Organometallics* **1996**, *15*, 2373; e) V. K. Dioumaev, P. J. Carroll, D. H. Berry, *Angew. Chem. Int. Ed.* **2003**, *42*, 3947.

[4] a) M. Driess, H. Pritzkow, M. Reisgys, *Angew. Chem.* **1992**, *104*, 1514; *Angew. Chem. Int. Ed. Engl.* **1992**, *31*, 1510; b) M. Driess, H. Pritzkow, M. Reisgys, *Chem. Ber.* **1996**, *129*, 247.

[5] a) A. D. Sadow, T. D. Tilley, *J. Am. Chem. Soc.* **2003**, *125*, 9462; b) B. Mork, T. D. Tilley, *Angew. Chem.* **2003**, *115*, 371; *Angew. Chem. Int. Ed.* **2003**, *42*, 357; c) T. Watanabe, H. Hashimoto, H. Tobita, *Angew. Chem.* **2004**, *116*, 220; *Angew. Chem. Int. Ed.* **2004**, *43*, 218.

[6] a) G. I. Nikonov, L. G. Kuzmina, S. F. Vyboishchikov, D. A. Lemenovskii, J. A. K. Howard, *Chem. Eur. J.* **1999**, *5*, 2497; b) V. I. Bakhmutov, J. A. K. Howard, D. A. Keen, L G. Kuzmina, M. A. Leech, G. I. Nikonov, E. V. Vorontsov, C. C. Wilson, *J. Chem. Soc. Dalton Trans.* **2000**, 1631; c) G. I. Nikonov, L. G. Kuzmina, J. A. K. Howard, *J. Chem. Soc. Dalton Trans.* **2002**, 3037.

[7] a) G. I. Nikonov, P. Mountford, S. K. Ignatov, J. C. Green, P. A. Cooke, M. A. Leech, L. G. Kuzmina, A. G. Razuvaev, N. H. Rees, A. J. Blake, J. A. K. Howard, D. A. Lemenovskii, *Dalton Trans.* **2001**, 2903; b) S. R. Dubberley, S. K. Ignatov, N. H. Rees, A. G. Razuvaev, P. Mountford, G. I. Nikonov, *J. Am. Chem. Soc* **2003**, *125*, 642; c) G. I. Nikonov, P. Mountford, S. R. Dubberley, *Inorg. Chem.* **2003**, *42*, 258.

[8] T. I. Gountchev, T. D. Tilley, *J. Am. Chem. Soc.* **1997**, *119*, 12831.

[9] K. Hübler, U. Hübler, W. R. Roper, P. Schwerdtfeger, L. J. Wright, *Chem. Eur. J.* **1997**, *3*, 1608.

[10] a) K. Hussein, C. J. Marsden, J.-C. Barthelat, V. Rodriguesz, S. Coneiro, S. Sabo-Etienne, B. Donnadieu, B. Chaudret, *Chem. Commun.* **1999**, 1315; b) I. Atheaux, F. Delpech, B. Donnadieu, S. Sabo-Etienne, B. Chaudret, K. Hussein, J. C. Barthelat, T. Braun, S. B. Duckett, R. N. Perutz, *Organometallics* **2002**, *21*, 5347; c) I. Atheaux, B. Donnadieu, V. Rodriguez, S. Sabo-Etienne, B. Chaudret, K. Hussein, J.-C. Barthelat, *J. Am. Chem. Soc.* **2000**, *122*, 5664; d) F. Delpech, S. Sabo-Etienne, J.-C. Daran, B. Chaudret, K. Hussein, C. J. Marsden, J.-C. Barthelat, *J. Am. Chem. Soc.* **1999**, *121*, 6668.

[11] N. M. Yardy, F. R. Lemke, L. Brammer, *Organometallics* **2001**, *20*, 5670.

[12] G. I. Nikonov, *Angew. Chem.* **2001**, *113*, 3457; *Angew. Chem. Int. Ed.* **2001**, *40*, 3353.
[13] E. Spaltenstein, P. Palma, K. A. Kreutzer, C. A. Willoughby, W. M. Davis, S. L. Buchwald, *J. Am. Chem. Soc.* **1994**, *116*, 10308.
[14] a) L. Hao, A.-M. Lebuis, J. F. Harrod, *Chem. Commun.* **1998**, 1089; b) H. G.; Woo, J. F. Harrod, J. Hénique, E. Samuel, *Organometallics* **1993**, *12*, 2883; c) J. Britten, Y. Mu, J. F. Harrod, J. Polowin, M. C. Baird, E. Samuel, *Organometallics* **1993**, *12*, 2672; d) E. Samuel, Y. Mu, J. F. Harrod, Y. Dromzee, Y. Jeannin, *J.Am.Chem.Soc.* **1990**, *112*, 3435; e) C. Aitken, J. F. Harrod, E. Samuel, *J. Am. Chem. Soc.* **1986**, *108*, 4059.
[15] R. Shu, L. Hao, J. F. Harrod, H.-G. Woo, E. Samuel, *J. Am. Chem. Soc.* **1998**, *120*, 12988.
[16] N. Muhoro, X. M. He, J. F. Hartwig, *J. Am. Chem. Soc.* **1999**, *121*, 5033.
[17] D. Liu, K. C. Lam, Z. Lin, *Organometallics* **2003**, *22*, 2827.
[18] L. B. Kool, M. D. Rausch, H. G. Alt, M. Herberhold, B. Wolf, U. Thewalt, *J. Organomet. Chem.* **1985**, *297*, 159.
[19] a) J. E. Bercaw, R. H. Msarvich, R. H. Bell, H. H. Brintzinger, *J. Am. Chem. Soc.* **1972**, *94*, 1219; b) J. L. Bennet, P. T. Wolczanski, *J. Am. Chem. Soc.* **1994**, *116*, 2179; c) H. Noth, M. Schmidt, *Organometallics* **1995**, *14*, 4601; d) Z. K. Sweeney, J. L. Polse, R. A. Anderson, R. G. Bergman, M. G. Kubinec, *J. Am. Chem. Soc.* **1997**, *119*, 4543; e) A. W. Kaplan, J. L. Polse, G. E. Ball, R. A. Anderson, R. G. Bergman, *J. Am. Chem. Soc.* **1998**, *120*, 11649.
[20] a) J. M. de Wolf, A. Meetsma, J. H. Teuben, *Organometallics* **1995**, *14*, 5466; b) J. W. Pattiasina, F. Bolhius, J. H. Teuben, *Angew. Chem.* **1987**, *99*, 342; *Angew. Chem. Int. Ed. Engl.* **1987**, *26*, 330; c) J. H. Teuben, *Organometallics* **1991**, *10*, 3227; d) W. W. Lukens, Jr., P. T. Matsunaga, R. Andersen, *Organometallics* **1998**, *17*, 5240.
[21] a) D. L. Lichtenberger, *Organometallics* **2003**, *22*, 1599; b) G. I. Nikonov, *Organometallics* **2003**, *22*, 1597.
[22] *NMR and the Periodic Table* (Eds.: R. K. Harris, B. E. Mann), Academic Press, London, **1978**.
[23] H. A. Bent, *Chem. Rev.* **1961**, *61*, 275.
[24] The extent of Si–H oxidative addition depends on the extent of backdonation from the metal to the (Si–H)* antibonding orbital.[1a] Electronegative groups on silicon decrease the energy of (Si–H)* and thus promote more pronounced Si–H oxidative addition to metal. See refs. [1a–d]
[25] Literature data for $Si(OEt)_4$: ^{29}Si NMR chemical shift 82.4 ppm. R. K. Harris, B. J. Kimber, *Org. Magn. Reson.* **1975**, *7*, 460.
[26] a) J. Burgio, N. M. Yardy, J. L. Petersen, F. R. Lemke, *Organometallics* **2003**, *22*, 4928; b) N. M. Yardy, F. R. Lemke, L. Brammer, *Organometallics* **2001**, *20*, 5670; c) G. N. van Buuren, A. C. Willis, F. W. B. Einstein, L.K. Peterson, R. K. Pomeroy, D. Sutton, *Inorg. Chem.* **1981**, *20*, 4361; d) A. A. Zlota, F. Frolow, D. Milstein, *Chem. Commun.* **1989**, 1826; e) H. Yamashita, A. M. Kawamoto, M. Tanaka, M. Goto, *Chem. Lett.* **1990**, 2107; f) A. K. Roy, R. B. Taylor, *J. Am. Chem. Soc.* **2002**, *124*, 9510; g) U. Schubert, A. Rengstl *J. Organomet. Chem.* **1979**, *166*, 323; h) F. R. Lemke, R. S. Simons, W. J. Youngs, *Organometallics* **1996**, *15*, 216.
[27] S. R. Frerics, B. K. Stein, J. E. Ellis, *J. Am. Chem. Soc.* **1987**, *109*, 5558.
[28] Y. You, S. R. Wilson, G. S. Girolami, *Organometallics* **1994**, *13*, 4655.
[29] K. B. Wiberg, *Tetrahedron* **1968**, *24*, 1024.
[30] A. E. Reed, L. A. Curtiss, F. Weinhold, *Chem. Rev.* **1988**, *88*, 899.
[31] a) R. F. Bader, *Atoms in Molecules: A Quantum Theory*, Clarendon, New York, **1990**; b) D. Cremer, E. Kraka, *Angew. Chem.* **1984**, *96*, 627; *Angew. Chem. Int. Ed. Engl.* **1984**, *23*, 612; c) D. Cremer, E. Kraka, *Croat. Chem. Acta* **1984**, *57*, 1259.
[32] Large bond ellipticity for the M–H bond has been observed in some agostic species: a) W. Scherer, W. Hieringer, M. Spiegler, P. Sirsch, G. S. McGrady, A. J. Downs, A. Haaland, B. Pedersen, *Chem. Commun.* **1998**, 2471; b) W. Scherer, G. S. McGrady, *Angew. Chem.* **2004**, *116*, 1816; *Angew. Chem. Int. Ed.* **2004**, *43*, 1782.
[33] a) G. M. Sheldrick, SHELXS-86 Program for Crystal Structure Solution, *Acta Crystallogr. Sect. A* **1990**, *146*, 467; b) A. Altomare, G. Cascarano, G. Giacovazzo, A. Guagliardi, M. C. Burla, G. Polidori, M. Camalli, *J. Appl. Crystallogr.* **1994**, *27*, 435.
[34] G. M. Sheldrick, SHELXTL-96, Program for Crystal Structure Refinement, Universität Göttingen, **1996**.
[35] Gaussian 98 (Revision A.3), M. J. Frisch, G. W. Trucks, H. B. Schlegel, G. E. Scuseria, M. A. Robb, J. R. Cheeseman, V. G. Zakrzewski, J. A. Montgomery, Jr., R. E. Stratmann, J. C. Burant, S. Dapprich, J. M. Millam, A. D. Daniels, K. N. Kudin, M. C. Strain, O. Farkas, J. Tomasi, V. Barone, M. Cossi, R. Cammi, B. Mennucci, C. Pomelli, C. Adamo, S. Clifford, J. Ochterski, G. A. Petersson, P. Y. Ayala, Q. Cui, K. Morokuma, D. K. Malick, A. D. Rabuck, K. Raghavachari, J. B. Foresman, J. Cioslowski, J. V. Ortiz, B. B. Stefanov, G. Liu, A. Liashenko, P. Piskorz, I. Komaromi, R. Gomperts, R. L. Martin, D. J. Fox, T. Keith, M. A. Al-Laham, C. Y. Peng, A. Nanayakkara, C. Gonzalez, M. Challacombe, P. M. W. Gill, B. G. Johnson, W. Chen, M. W. Wong, J. L. Andres, M. Head-Gordon, E. S. Replogle, J. A. Pople, Gaussian, Inc., Pittsburgh, PA, **1998**.
[36] P. J. Hay, W. R. Wadt, *J. Chem. Phys.* **1985**, *82*, 299.
[37] A. Bergner, M. Dolg, W. Kuechle, H. Stoll, H. Preuss, *Mol. Phys.* **1993**, *80*, 1431; U. Wedig, M. Dolg, H. Stoll, H. Preuss in *Quantum Chemistry: The Challenge of Transition Metals and Coordination Chemistry.* (Ed.: A. Veillard), Reidel, Dordrecht, **1986**, p. 79.

Received: March 10, 2004
Revised: May 25, 2004
Published online: August 23, 2004

